Catalysis Today 179 (2012) 130–139

Contents lists available at ScienceDirect

Catalysis Today

journal homepage: www.elsevier.com/locate/cattod

Zirconocene silanolate complexes and their heterogeneous siliceous analogues as catalysts for phenylsilane dehydropolymerization

Vojtech Varga [a], Michal Horáček [b], Zdeněk Bastl [b], Jan Merna [c], Ivana Císařová [d], Jan Sýkora [e], Jiří Pinkas [b,*]

[a] Research Institute of Inorganic Chemistry, a.s., Revoluční 84, 400 01 Ústí nad Labem, Czech Republic
[b] J. Heyrovský Institute of Physical Chemistry of ASCR, v.v.i., Dolejškova 2155/3, 182 23 Prague 8, Czech Republic
[c] Institute of Chemical Technology, Prague, Department of Polymers, Technická 5, 166 28 Prague 6, Czech Republic
[d] Charles University, Department of Inorganic Chemistry, Hlavova 2030, 128 43, Prague 2, Czech Republic
[e] Institute of Chemical Process Fundamentals of ASCR, v.v.i., Rozvojová 135, 165 02 Prague 6, Czech Republic

ARTICLE INFO

Article history:
Received 26 May 2011
Received in revised form 29 June 2011
Accepted 1 July 2011
Available online 4 August 2011

Keywords:
Catalysis
Dehydrocoupling
Polysilanes
Supported metallocenes
Silanolate
Silica

ABSTRACT

The efficient catalytic dehydropolymerization of phenylsilane by homogeneous zirconocene bissilanolates ([{(c-C_5H_9)$_7$$Si_8O_{12}O$}$_2$Zr($\eta^5$-$C_5H_5$)$_2$] (**1a**); [{(c-$C_5H_9$)$_7$$Si_8O_{12}O$}$_2$Zr($\eta^5$-$C_5H_4Bu$)$_2$] (**1b**) [{(*c*-$C_5H_9$)$_7$$Si_7O_9$(OSiMe$_3$)$O_2$}Zr($\eta^5$-$C_5H_5$)$_2$] (**4**); [{($Me_3CO$)$_3$SiO}$_2$Zr($\eta^5$-$C_5H_5$)$_2$] (**5**)) and chlorosilanolates ([{(c-C_5H_9)$_7$$Si_8O_{12}O$}ZrCl($\eta^5$-$C_5H_4Bu$)$_2$] (**2**); ([{(*c*-$C_5H_9$)$_7$$Si_7O_9O_3$}$Zr_2$Cl($\eta^5$-$C_5H_5$)$_4$] (**3a**); [{(*c*-$C_5H_9$)$_7$$Si_7O_9O_3$}$Zr_2$Cl($\eta^5$-$C_5H_4Bu$)$_4$] (**3b**)) has been demonstrated. The presence of at least one silanol ligand in the zirconocene moiety was found essential for high catalytic performance. Solid state structure of complex **1a** was determined by single crystal X-ray diffraction analysis. A series of nine zirconocene-siliceous catalysts were prepared by grafting of zirconocene moiety onto silica using three general methods: (a) reaction of [(η^5-C_5H_5)$_2$$ZrCl_2$] with silica in the presence of NEt_3; (b) reaction of [(η^5-C_5H_5)$_2$$ZrMe_2$] with silica; (c) reaction of solely [(η^5-C_5H_5)$_2$$ZrCl_2$] with silica. Supported catalysts were characterized by ICP-MS, FT-IR, TGA and selected examples by XPS analysis. Those catalysts prepared by method (a) and (b) were found efficient in the phenylsilane polymerization although a higher Zr/monomer ratio had to be used in comparison with homogeneous analogues. The low concentration of residual silanol groups in supported catalysts was found essential for their high catalytic performance. Advantageous reusability of supported catalysts was demonstrated using $SiO_{2(500)}$/Cp_2ZrCl_2/NEt_3(5.8). The catalytic performance was retained in three consecutive cycles producing polymers with almost identical properties.

1. Introduction

Extraordinary properties of polysilanes due to their σ-electron delocalization conjugation have been applied in design of new ceramics, semiconductor, photoresistive and non-linear optic materials [1,2]. Polysilanes preparation by group 4 complexes catalyzed dehydrocoupling of hydrosilanes become a feasible alternative to Wurtz coupling of chlorosilanes and has been repeatedly reviewed [3–5]. The high activity of [(η^5-C_5H_5)$_2$$TiMe_2$] [6] and [($\eta^5$-$C_5H_5$)$_2$$ZrMe_2$] [7] in catalytic silane dehydrocoupling led to the exploration of the range of complexes with reactive alkyl or silyl groups σ-bonded to the metal [8,9]. The reactive metal–carbon or metal–hydrogen species could be also generated *in situ* from commercially available metallocene dichlorides by various alkylating/hydrogenating reagents (BuLi [10,11], $NaAlH_2(OC_2H_4OCH_3)_2$ [12]), however this method produced complicated mixtures of organometallic species [13]. In the mid nineties, the family of successful catalysts was extended for stable titanocenes bearing Ti–O bonds [(η^5-C_5H_5)$_2$Ti(OAr)$_2$] (Ar = Ph, 4-$MeOC_6H_4$, 4-Cl-C_6H_4, 4-CNC_6H_4, 4-Me-C_6H_4) [14,15] or stable metallocene fluorides [(η^5-C_5H_5)$_2$$MF_2$] (M = Ti, Zr) [16], respectively. Replacement of metal bonded σ-ligands with hydride transferred from silane was shown to be the activation step for dehydrocoupling polymerization of silanes with metallocenes [(η^5-C_5H_5)$_2$$MY_2$] (M = Ti, Zr, Hf; Y = F, OPh, NMe_2) [17]. The strength of the M-Y bond thus became an important factor for determination of effectiveness of ligand Y leaving process. Evaluation of ligand to metal π-donor ability in a series of titanocene complexes [(η^5-C_5Me_5)$_2$MY] introduced by Andersen for Y = N(Me)H, NH_2, OMe, OPh, F, Cl, Br, I, H [18] and recently extended to permethyltitanocene alcoholates and silanolates [19,20] established a valuable parameter for the ligand behaviour. The results obtained classified the π-interaction of silanolate ligands to be intermediate between those of phenolate and fluoride ligand. Assuming that silanol ligands could mimic the behaviour of silica surface silanol groups ("the surface (of silica) acts as a large siloxy ligand" [21]), there is a great potential

* Corresponding author.
E-mail address: pinkas@jh-inst.cas.cz (J. Pinkas).

0920-5861/$ – see front matter © 2011 Elsevier B.V. All rights reserved.
doi:10.1016/j.cattod.2011.07.006

in use of metallocene complexes grafted on silica to catalyze the dehydrocoupling polymerization of primary silanes. Although the zirconocenes grafted on silica were extensively studied as precursors for catalytic polymerization of olefins (especially ethylene) [22–24], there has been no study concerning their use for dehydrogenative polymerization of primary silanes.

In this contribution we compare the catalytic performance of homogeneous zirconocene–silanolate complexes **1**–**5** (Chart 1) in dehydrocoupling polymerization of phenylsilane with new heterogeneous zirconocene–siliceous complexes containing a diverse Zr loading. The effect of the heterogeneous catalyst composition on catalytic dehydrocoupling polymerization of phenylsilane and on properties of the polymers obtained is evaluated. The reusability of particular heterogeneous catalysts is also examined.

2. Materials and methods

2.1. Materials

All manipulation with moisture- and air-sensitive compounds were carried out under argon (99.998%) using standard Schlenk techniques or in a glovebox Labmaster 130 (mBraun) under purified nitrogen. Solvents were dried, and freshly distilled prior to use. $[(\eta^5\text{-}C_5H_5)_2ZrCl_2]$, $[(\eta^5\text{-}C_5H_5)_2ZrMe_2]$ were obtained from Aldrich and used as received. NEt_3 (Fluka) was dried by refluxing over Na/benzophenone, distilled and stored over a Na mirror. Phenylsilane (Fluka) was dried by refluxing over $LiAlH_4$ prior to distillation. *Caution: Prolonged reflux of $PhSiH_3$ with $LiAlH_4$ generates SiH_4 (a self-igniting gas).*

Homogeneous zirconocene complexes were prepared according to literature procedures: **1**–**3** [25], **4** [26,27], **5** [28].

Silica (Purasil 60 Å, 70–230 mesh, Whatman, BET surface area 539 m^2/g, pore volume 0.8 cm^3/g and average pore diameter 5.2 nm) was dried under a dynamic vacuum (10^{-3} Torr) for 10 h at 200 °C (denoted $SiO_{2(200)}$) or 500 °C (denoted $SiO_{2(500)}$), respectively. Content of residual silanol groups on the silica surface was determined by TGA to be 3.6 mmol –OH groups/g $SiO_{2(200)}$ and 0.7 mmol –OH groups/g $SiO_{2(500)}$.

2.2. Characterization methods

^1H (300.0 MHz) and ^{13}C (75.4 MHz) NMR spectra of soluble products from heterogeneous catalyst preparation were recorded on a Varian Mercury 300 spectrometer at 25 °C. Chemical shifts (δ/ppm) are given relative to solvent signals (C_6D_6: δ_H 7.15 ppm, δ_C 128.00 ppm; $CDCl_3$: δ_H 7.26 ppm, δ_C 77.16 ppm). ^1H and ^{29}Si NMR spectral measurements of phenylsilane dehydrocoupling catalyzed with **1a** were performed on a Varian UNITY-500 spectrometer (operating at 499.9 MHz for ^1H and 99.3 MHz for ^{29}Si nucleus) at 20 °C. The $^{29}Si\{^1H\}$ INEPT based on $^1J(^{29}Si–^1H) \sim 200$ Hz was performed with relaxation delay 3 s and acquisition time of 2 s. ^1H NMR (499.9 MHz) of poly(phenyl)silanes were recorded on a Varian UNITY-500 spectrometer in $(CD_3)_2CO$ (referenced to residual solvent signal at δ_H 2.05 ppm).

GC–MS of volatile products were measured with Thermo Focus DSQ instrument using the capillary column Thermo TR-5MS (15 m × 0.25 mm ID × 0.25 mm).

X-ray diffraction data for **1a** were collected at 150 K on a Nonius KappaCCD diffractometer (Enraf-Nonius) with the graphite monochromated Mo-Kα radiation. Cryostream Cooler (Oxford Cryosystem) was used for the low temperature measurements. The structure was solved by direct methods (SHELXL97) [29] and refined by full-matrix least-squares on F^2 values (CRYSTALS) [30]. The assymetric unit of the crystal lattice contains a single zirconocene molecule. It was inevitable to model the disorder of the three cyclopentyl groups. All heavy atoms and the carbon atoms with the full occupancies were refined anisotropically. The disordered carbon atoms were refined only isotropically. Hydrogen atoms were localized from the expected geometry and were not refined. The crystallographic data for the structures reported in this paper have been deposited with the Cambridge Crystallographic Data Centre as supplementary data. Copies of the data can be obtained free of charge on application to CCDC, e-mail: deposit@ccdc.cam.ac.uk.

Crystallographic data for **1a**: $C_{80}H_{136}O_{26}Si_{16}Zr_1$, M= 2054.5 g/mol, monoclic system, space group $P2_1/c$, a = 11.4376(2), b = 22.5375(4), c = 38.8822(6) Å, β = 93.972(8)°, Z = 4, V = 9998.8(3) Å^3, Dc = 1.36 g cm^{-3}, μ(Mo Kα) = 0.37 mm^{-1}, T = 150 K, crystal dimensions of 0.06 mm × 0.25 mm × 0.40 mm. The structure converged to the final R = 0.0865 and R_w = 0.0967 using 7392 independent reflections (θ_{max} = 25.02°). CCDC registration number 826482.

The zirconium content in heterogeneous complexes was determined by Inductively Coupled Plasma–Mass Spectrometer (ICP–MS) Perkin Elmer Elan 6000. Samples were dissolved in concentrated hydrofluoric and nitric acids with the aid of microwave equipment.

IR spectra of heterogeneous catalysts were taken as a nujol mull between KBr plates on a Nicolet Avatar FTIR spectrometer in the range 400–4000 cm^{-1}

Thermal analyses (TGA) of heterogeneous complexes were performed on a TGA Q500 (TA Instruments, USA) under a nitrogen flow (60 ml min^{-1}) with temperature programming of 20 °C min^{-1}. The initial weight loss up to ca. 160 °C should be attributed to removal of water physisorbed during the sample weighting.

XPS analyses of heterogeneous complexes were carried out using VG ESCA3 MkII electron spectrometer equipped with an Al Kα X-ray source and electrostatic hemispherical electron analyzer. Spectra were taken at low resolution in the range 0–1000 eV and in high resolution mode for the Si 2p, Zr 3d, Cl 2p, C 1s regions. The measured core level binding energies Zr $3d_{5/2}$ are given relative to Si 2p line located at 103.4 eV and the estimated error in binding energy determination was ±0.2 eV. Element concentration ratios were calculated from the photoelectron peak areas after their correction for non-linear Shirley background. The estimated error in obtained values was ±10%.

Molar masses of polysilanes were determined on a Waters Breeze chromatographic system (Waters 2410 refractive index detector, Waters 1515 pump, Waters 717plus Autosampler, column heater) with RI detector operating at 880 nm and multi-angle laser light scattering (MALLS) miniDawn TREOS from Wyatt with laser wavelength 658 nm. Refractive index increments (dn/dc = 0.238–0.268 ml g^{-1}) were measured on-line on RI detector at 880 nm. Separation was performed on two 7.8 mm × 300 mm Polymer Laboratories Mixed C columns at 35 °C in THF at an elution rate of 1 ml min^{-1}. Samples concentration was 3–5 mg ml^{-1}. Light scattering data were evaluated using Astra 5.3.2.15 software. The amount of LMW fraction was evaluated from the deconvolution of GPC chromatogram of the respective polysilane. Note: Selected samples were also evaluated using polystyrene calibration which on average resulted in approximately 30% underestimation of M_w compared to results from GPC-MALLS.

2.3. Phenylsilane polymerization with homogeneous complexes **1**–**5**

Polymerizations were performed in a Schlenk tube under argon atmosphere. Phenylsilane (1.080 g, 10 mmol) was added to a solid zirconocene complex (10 μmol Zr) and the mixture was stirred for 15 h in an oil bath heated to 105 °C. The resulting glass/oily material was dissolved in 15 ml of toluene. The toluene solution was filtered

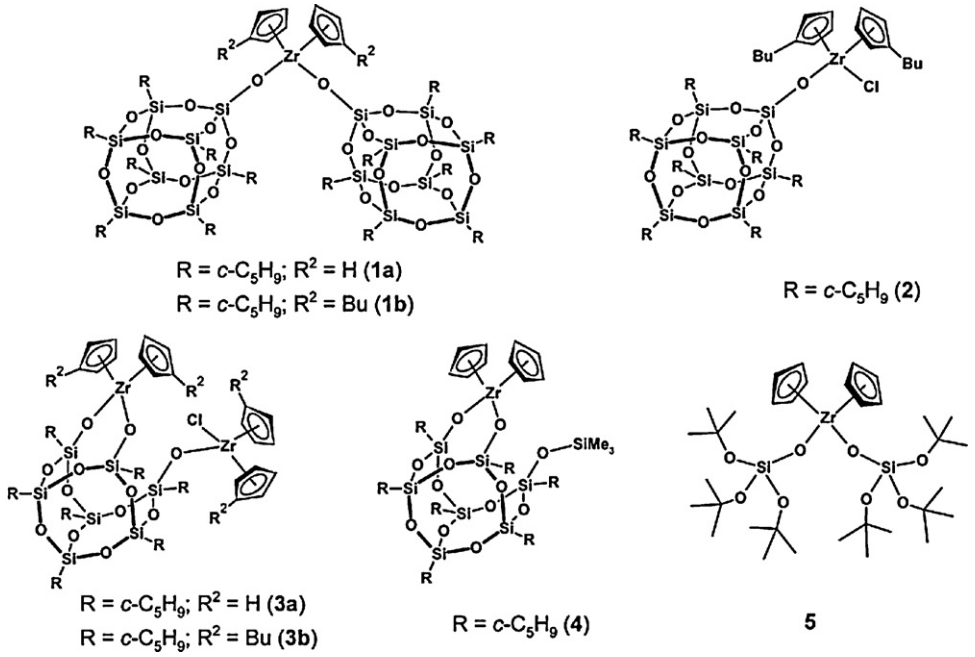

Chart 1.

through Florisil and the solid phase washed with toluene (3× 5 ml). Combined toluene fractions were evaporated in vacuum to obtain polymers of oil-to-glass appearance.

Complexes with *n*-butyl substituted zirconocene moiety (**1b**, **2**, **3b**) were activated at 135 °C for 30 min, and the polymerization was further conducted at 105 °C for additional 14.5 h.

2.4. ^1H NMR spectroscopy of a mixture of **1a** and $PhSiH_3$

Complex **1a** (6 mg, 3 μmol) was weighed into a high-pressure NMR tube, and an excess of phenylsilane (372 μl, 327 mg, 3.0 mmol) was added with a Hamilton syringe. The resulting suspension was degassed, closed with a J-Young valve, and initial ^1H and ^{29}Si NMR spectra were acquired. The dehydrocoupling reaction was initiated by heating the tube for 20 min at 110–120 °C. Then the tube was cooled to room temperature and the reaction was periodically monitored by ^1H and ^{29}Si NMR measurement for 15 h. Hereupon leaving the NMR tube for several days at room temperature led to formation of colourless crystals. These were isolated and showed by X-ray crystallography to be **1a**.

2.5. Preparation of heterogeneous zirconocenes supported on silica

Method A: from $[(\eta^5\text{-}C_5H_5)ZrCl_2]$ with NEt_3 as a base (given an example for $SiO_{2(500)}/Cp_2ZrCl_2/NEt_3(5.8)$).

To a solid mixture of silica $SiO_{2(500)}$ (1.980 g) and $[(\eta^5\text{-}C_5H_5)_2ZrCl_2]$ (0.485 g, 1.66 mmol) was added chloroform (70 ml), followed by an excess of NEt_3 (2.0 ml, 14.3 mmol). The mixture was stirred at room temperature for 20 h. Then, the solid part was separated from a colourless solution, washed with chloroform (3× 10 ml) and THF (10 ml), and dried in vacuum to give a slightly yellow solid (2.243 g) denoted as $SiO_{2(500)}/Cp_2ZrCl_2/NEt_3(5.8)$. The parentheses indicate the loading of Zr in weight % (see entry 2 in Table 2). The reaction solution and all washings were combined, and evaporated to dryness to obtain a white solid (0.323 g). The ^1H NMR analysis revealed the presence of $[Et_3NH]Cl$ with traces (<0.5 mol.%) of $[\{(\eta^5\text{-}C_5H_5)_2ZrCl\}_2O]$ (^1H NMR ($CDCl_3$): δ_H = 6.29 ppm) [31].

Table 1
Dehydrogenative polymerization of phenylsilane catalyzed with homogeneous complexes **1**–**5** and $[(\eta^5\text{-}C_5H_5)_2ZrCl_2]$. Conditions: $Zr/PhSiH_3$ = 1/1000; temp. = 105 °C; time = 15 h; neat $PhSiH_3$.

Entry	Catalyst	Conv. [%]	M_w[a] [kg mol^{-1}]	D[a,b]	LMF[a,c] [mol%]
1	1a	96	1.96	1.45	16
2	1b[d]	98	1.74	1.37	16
3	2[d]	90	3.60	1.79	10
4	3a	95	3.58	1.68	13
5	3b[d]	85	2.31	1.41	10
6	4	83	2.20	1.42	18
7	5	82	2.80	1.64	14
8	$[(\eta^5\text{-}C_5H_5)_2ZrCl_2]$	0	–	–	–

[a] Determined by GPC-MALLS.
[b] Dispersity $D = M_w/M_n$
[c] Low molecular weight fraction.
[d] Catalyst activation was performed at 135 °C (for 30 min).

Method B: from $[(\eta^5\text{-}C_5H_5)_2ZrMe_2]$ (given an example for $SiO_{2(200)}/Cp_2ZrMe_2(9.5)$).

Toluene (15 ml) was added to a solid mixture of silica $SiO_{2(200)}$ (0.978 g) and $[(\eta^5\text{-}C_5H_5)_2ZrMe_2]$. A vigorous gas evolution and warming of the reaction mixture was observed. The mixture was stirred at room temperature for additional 12 h. The solution was filtered, and the solid residue was washed with toluene (3× 5 ml) and dried under vacuum to obtain a supported catalyst as a yellowish solid (1.243 g).

The filtrate and washings were combined and evaporated in vacuum to obtain a waxy yellowish solid (0.104 g). The analysis of the solid by ^1H NMR (C_6D_6) showed mainly the presence of unreacted $[(\eta^5\text{-}C_5H_5)_2ZrMe_2]$ (ca. 80 mol.%).

Method C: from $[(\eta^5\text{-}C_5H_5)_2ZrCl_2]$ without base (given an example for $SiO_{2(500)}/Cp_2ZrCl_2(0.8)$).

A solution of $[(\eta^5\text{-}C_5H_5)_2ZrCl_2]$ (0.085 g, 0.29 mmol) in toluene (10 ml) was added to silica $SiO_{2(500)}$ (0.997 g) and the mixture was stirred at room temperature for 17 h. The solution was filtered, and the remaining solid was washed with toluene (4× 5 ml) and dried in vacuum for 5 h. The filtrate and washings were collected and evaporated under vacuum. The solid residue was analyzed by

Table 2
Dehydrogenative polymerization of phenylsilane catalyzed with heterogeneous catalysts. Conditions: $Zr/PhSiH_3 = 1/100$; temp. = 105 °C; time = 15 h; neat $PhSiH_3$.

Entry	Catalyst (Zr wt%)[a]	Conv. [%]	M_w[b] [kg mol^{-1}]	D[b,c]	LMF[b,d] [mol%]
1	$SiO_{2(500)}/Cp_2ZrCl_2/NEt_3$(5.3)	90	4.01	1.78	10
2	$SiO_{2(500)}/Cp_2ZrCl_2/NEt_3$(5.8)	91	3.70	1.69	9
3	$SiO_{2(500)}/Cp_2ZrCl_2/NEt_3$(3.0)	81	3.61	1.64	10
4	$SiO_{2(500)}/Cp_2ZrCl_2/NEt_3$(3.0)	69	3.96	1.73	10
5	$SiO_{2(200)}/Cp_2ZrCl_2/NEt_3$(7.8)	45	1.20	2.22	68
6	$SiO_{2(200)}/Cp_2ZrCl_2/NEt_3$(8.7)	42	0.89	1.31	100
7	$SiO_{2(500)}/Cp_2ZrMe_2$(7.5)	93	2.40	1.41	22
8	$SiO_{2(200)}/Cp_2ZrMe_2$(9.5)	91	3.34	1.57	13
9	$SiO_{2(500)}/Cp_2ZrCl_2$(0.8)	0	–	–	–
10	$SiO_{2(200)}/Cp_2ZrCl_2$(1.1)	0	–	–	–

[a] Determined by ICP-MS.
[b] Determined by GPC-MALLS.
[c] Dispersity $D = M_w/M_n$.
[d] Low molecular weight fraction.

^{1}H NMR to be solely unreacted [(η^5-C_5H_5)$_2ZrCl_2$] ($CDCl_3$: signal at δ_H = 6.49 ppm).

2.6. Phenylsilane polymerization with heterogeneous complexes

Polymerizations were performed in a Schlenk tube under an argon atmosphere. Phenylsilane (1.080 g, 10 mmol) was added to a grafted catalyst (0.10 mmol Zr) and the mixture was inserted into a bath heated to 105 °C and stirred for 15 h. The polysilane formed was dissolved in toluene (usually ca. 20 ml) and the toluene solution was filtered from the solid catalysts. The catalyst was washed with additional portions of toluene (3 × 5 ml). Combined toluene fractions were evaporated in vacuum to obtain a colourless or slightly yellow polymer of oil-to-glass appearance.

2.7. Reaction of neat $PhSiH_3$ with silica (given an example for $SiO_{2(200)}/PhSiH_3$)

A mixture of silica $SiO_{2(200)}$ (0.796 g) and $PhSiH_3$ (1.756 g, 16.26 mmol) was heated to 105 °C and stirred for 15 h. Then, the liquid phase was separated and the remaining solid was dried under vacuum to obtain a white surface-modified silica $SiO_{2(200)}/PhSiH_3$ (yield 0.887 g).

Similarly, a modified silica $SiO_{2(500)}/PhSiH_3$ (yield 0.354 g) was prepared from silica $SiO_{2(500)}$ (0.320 g) and $PhSiH_3$ (0.878 g, 8.13 mmol).

GC–MS analysis of volatiles from both preparations proved the presence of benzene in addition to overwhelming $PhSiH_3$.

3. Results and discussion

3.1. Catalytic phenylsilane polymerization by homogeneous complexes ***1–5***

Dehydrocoupling phenylsilane polymerizations with zirconocene complexes **1**–**5** (Chart 1) were performed at 105 °C in bulk monomer ($Zr/PhSiH_3 = 1/1000$; n/n). Polymerization conditions, conversions and GPC characterization of obtained polysilanes are summarized in Table 1. The polymerization commenced within 10–30 min and could be visually detected by hydrogen evolution and in some cases by colour change from colourless to yellowish. During this prerequisite activation a catalytic active species should be generated from the particular complex by replacing σ-bonded ligand(s) with hydride transferred from silane [17]. The catalytic performance of bis(silanolate) complexes was only slightly higher in comparison to chlorosilanolates, whereas [(η^5-C_5H_5)$_2ZrCl_2$] was inactive at the same conditions showing that the silanolate ligand behaves as a better leaving group than the chloride ligand. A similar relation was found for catalytic dehydrocoupling of phenylsilane with titanocene complexes bearing aryloxo and chloro σ-ligands [32]. It should be noted, that complexes with the *n*-butyl substituted zirconocene moiety (**1b**, **2**, **3b**) required higher activation temperature (135 °C in bath) to commence the polymerization, probably as a result of higher steric crowding at the zirconium centre. Once the polymerization started, the catalytic performance of zirconocene (conversion 82–96%) and *n*-butyl substituted zirconocene species (conversion 85–98%) was almost identical, showing only negligible effect of cyclopentadienyl monosubstitution on catalytic performance.

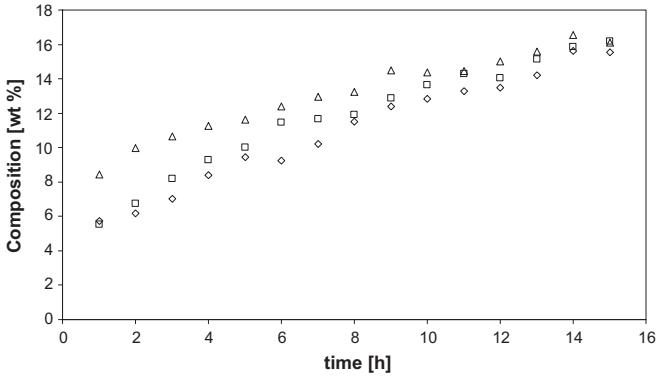

Fig. 1. Proceeding of phenylsilane polymerization catalyzed with **1a**. $H_2PhSi(SiHPh)SiPhH_2$ (Δ); $H_2PhSi(SiHPh)_2SiPhH_2$ (2 diastereomers: (□) and (◊)).

GPC-MALLS analysis of polysilanes prepared with **1**–**5** showed a bimodal distribution of molecular weight (M_w in the range 1.74–3.60 kg mol^{-1}) with a low molecular weight fraction (LMW) in the range 10–18%. The M_w values of polymers prepared by complexes with unsubstituted zirconocene moiety are similar (M_w = 1.96 (**1a**); 3.58 (**3a**); 2.20 (**4**) and 2.80 (**5**) kg mol^{-1}) to polymers obtained using catalytic systems: [(η^5-C_5H_5)$_2ZrCl_2$]/2, e.g. BuLi (M_w = 1.78–2.50 kg mol^{-1}) [10] and [(η^5-C_5H_5)$_2ZrY_2$] (Y = F, OPh, NMe_2; M_w = 2.70-3.14 kg mol^{-1}) [17].

An attempt to catalyze polymerization of silane Ph_2SiH_2 by complex **1a** was unsuccessful even at 135 °C showing limited activity of studied complexes towards secondary silanes.

3.2. ^{1}H and ^{29}Si NMR monitoring of phenylsilane polymerization with ***1a***

Replacement of the electronegative ligand Y (Me, F, OPh, NMe_2) σ-bonded to zirconium with hydride is to be accompanied by the formation of new silane species $PhSiH_2Y$ as was shown by Wang et al. [17]. To establish the similar reaction for silanolate ligands we have attempted to follow the activation of **1a** and subsequent catalytic phenylsilane polymerization by ^{1}H NMR spectroscopy. Unfortunately, a mixture of **1a** and phenylsilane in *o*-xylene-D_{10} did not show any activation even at 140 °C therefore the measurements were performed in neat phenylsilane. The dehydrocoupling commenced after short activation at 110–120 °C and formation of trimer $H_2PhSi(SiHPh)SiPhH_2$ and two diastereotopes for tetramer $H_2PhSi(SiHPh)_2SiPhH_2$ was detected by ^{29}Si NMR after further 1 h at room temperature. The ^{29}Si{^{1}H} INEPT with the refocusing delay corresponding to SiH group (0.0025 s) was collected every hour. The isolated *Si*H signals of the trisilane and tetrasilanes [33] were chosen to monitor the course of the reaction.

Fig. 1 shows slow increase in the concentration of monitored oligomers with time, thus supporting the proceeding dehydrocoupling. It should be noted that both diastereomers of the tetramer $H_2PhSi(SiHPh)_2SiPhH_2$ were produced with roughly equal

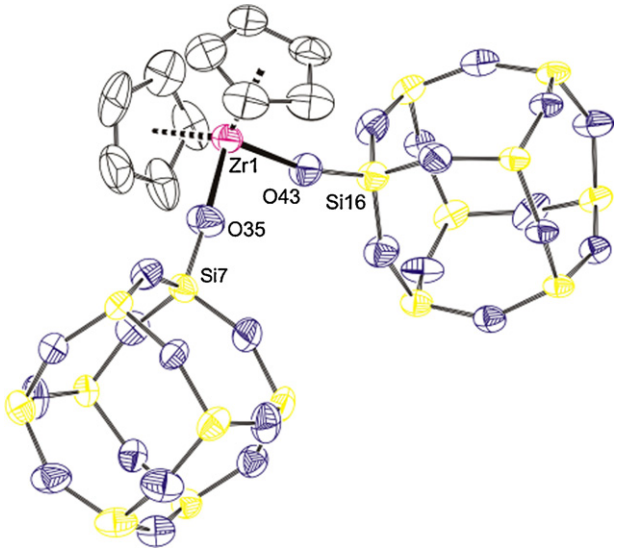

Fig. 2. ORTEP drawing of compound **1a** at the 30% probability level (cyclopentyl groups and hydrogen atoms are omitted for clarity). Selected bond distances (Å) and angles (°): Zr(1)–O(35) 1.981(7), Zr(1)–O(43) 1.967(7), Zr(1)–Cg(1) 2.220, Zr(1)–Cg(2) 2.209, O(43)–Zr(1)–O(35) 99.2(3), Zr(1)–O(43)–Si(16) 166.2(5), Zr(1)–O(35)–Si(7) 172.2(5).

abundance showing no stereoselectivity of the polymerization process. We were not able to detect any evidence for active hydride species or for $PhSiH_2$ modified silsequioxane. Moreover, a substantial amount of complex **1a** crystallized from the polymerization mixture after several days. Since attempted crystallization of **1a** from hexane afforded only a polycrystalline powder one could suggest that the formation of single crystals was due to a slow decrease of **1a** solubility in the produced oligomers. On the other hand, recovery of **1a** implies that activation process is rather ineffective and produces only small amount of active species which catalyze the dehydrocoupling highly effectively even at room temperature. It is probable that low concentration of the active species in the polymerization mixture lowered its deactivation by bimolecular reaction producing dimers inactive in dehydrocoupling polymerization [7,34].

3.3. Crystal structure of *1a*

The molecular structure of **1a** is depicted in Fig. 2. The central zirconium atom possesses approximately tetrahedral coordination environment consisting of the centroid of the two cyclopentadienyl rings and two oxygen atoms. Zr–O σ-bond distances have lengths (1.981(7) Å and 1.967(7) Å) comparable to known zirconocene complexes $[(\eta^5\text{-}C_5H_5)_2Zr\{(c\text{-}C_5H_9)_7Si_7O_{11}(OSiMe_3)\}]$ (1.96(2) Å) [26] and $[(\eta^5\text{-}C_5H_5)_2Zr\{(c\text{-}C_5H_9)_7Si_7O_{11}(OSiMePh_2)\}]$ (1.994(2) Å and 1995(2) Å) [27]. On the other hand, the Zr–O–Si angle (166.5(5)° and 172.5(5)°) in **1a** is considerably closer to linear arrangement than in above mentioned complexes (157.6(9)°, 155.9(10) in $[(\eta^5\text{-}C_5H_5)_2Zr\{(c\text{-}C_5H_9)_7Si_7O_{11}(OSiMe_3)\}]$ and 146(8(1)°, 161.4(1)° in $[(\eta^5\text{-}C_5H_5)_2Zr\{(c\text{-}C_5H_9)_7Si_7O_{11}(OSiMePh_2)\}]$ with chelating silsequioxane ligand, apparently due to a lower steric strain for monodentately bonded silsequioxane ligands in **1a**.

3.4. Heterogeneous catalyst preparation

Heterogeneous analogues of zirconocene silanolate complexes were prepared by reaction of $[(\eta^5\text{-}C_5H_5)_2ZrCl_2]$ or $[(\eta^5\text{-}C_5H_5)_2ZrMe_2]$ with partially dehydroxylated silica ($SiO_{2(200)}$, $SiO_{2(500)}$). Three general pathways were used for supporting the zirconocene moiety onto silica surface.

Method A: The utilization of NEt_3 as a base in the reaction of $[(\eta^5\text{-}C_5H_5)_2ZrCl_2]$ with surface silanol groups led to grafting of zirconocene moiety to the silica surface by at least one ≡SiO–Zr bond as was evidenced by the ammonium salt $[NEt_3H]Cl$ formation (*vide infra*). The content of the zirconium grafted on silica surface depends on a number of surface silanol groups and initial Zr/surface –OH ratio. Reaction of $[(\eta^5\text{-}C_5H_5)_2ZrCl_2]$ with $SiO_{2(200)}$ (3.6 mmol OH/g) at approximately Zr/OH = 0.5 gave supported catalyst $SiO_{2(200)}/Cp_2ZrCl_2/NEt_3(7.8)$ with 7.8 wt% Zr. Repeated experiment at identical conditions led to a supported catalyst $SiO_{2(200)}/Cp_2ZrCl_2/NEt_3(8.7)$ with slightly higher Zr content (8.7 wt% Zr). Reaction of $[\eta^5\text{-}C_5H_5)_2ZrCl_2]$ with $SiO_{2(500)}$ (0.7 mmol OH/g) at approximately Zr/OH = 1 gave supported catalyst $SiO_{2(500)}/Cp_2ZrCl_2/NEt_3(5.8)$ with 5.8 wt% of Zr. An increased zirconocene content in the reaction mixture (Zr/OH = 5) did not lead to a higher incorporation of zirconium and catalyst $SiO_{2(500)}/Cp_2ZrCl_2/NEt_3(5.3)$ with almost identical Zr content (5.3 wt%) was obtained. On the other hand, the use of low zirconocene content (Zr/OH = 0.5) in the reaction mixture led to the supported catalyst with $SiO_{2(500)}/Cp_2ZrCl_2/NEt_3(3.0)$ with 3 wt% Zr.

^1H NMR spectrum of filtrates + washings in $CDCl_3$ isolated from the reaction mixtures: silica + $[(\eta^5\text{-}C_5H_5)_2ZrCl_2]$ + NEt_3 showed besides signals corresponding to quaternary ammonium salt (characteristic broad signal of NH at 12.0 ppm) and in some cases unreacted $[(\eta^5\text{-}C_5H_5)_2ZrCl_2]$ (δ_H = 6.46 ppm) as well as a singlet at 6.29 ppm. The signal was assigned to μ-oxo dimer $[\{(\eta^5\text{-}C_5H_5)_2ZrCl\}_2O]$ [31]. The amount of the μ-oxo species varied from 0 to 4 mol.% respective to an amount of ammonium salt formed. A partial base catalyzed dehydroxylation of the silica surface and reaction of the *in situ* formed water with the zirconocene dichloride in the presence of NEt_3 is probably responsible for the formation of μ-oxo dimer $[\{(\eta^5\text{-}C_5H_5)_2ZrCl\}_2O]$. Analogous dehydratation of $[(c\text{-}C_5H_9)_7Si_7O_9(OH)_3]$ catalyzed by NEt_3 with either $[(\eta^5\text{-}C_5H_5)_2ZrCl_2]$ or MS 4A as water scavengers have already been published [25,35].

Method B To avoid problem with released water mentioned above we have used $[(\eta^5\text{-}C_5H_5)_2ZrMe_2]$ as a precursor for grafting zirconocene moiety on the silica surface. The complex contained highly reactive Zr–C bonds capable of interacting with weakly acidic surface silanol groups with a concomitant methane release. Such reactions in toluene suspension gave supported catalysts $SiO_{2(200)}/Cp_2ZrMe_2(9.5)$ and $SiO_{2(500)}/Cp_2ZrMe_2(7.5)$ with 9.5 and 7.5 wt% of Zr.

Method C: The method followed the preparation of ethene polymerization precatalysts as was described previously [36–39]. The thermally pretrated silicas $SiO_{2(200)}$ and $SiO_{2(500)}$ were admixed with toluene solution of $[(\eta^5\text{-}C_5H_5)_2ZrCl_2]$ for desired time, washed and dried in vacuum to obtain supported catalysts $SiO_{2(200)}/Cp_2ZrCl_2(1.1)$ or $SiO_{2(500)}/Cp_2ZrCl_2(0.8)$ with 1.1 or 0.8 weight % of zirconium, respectively. The rather low zirconium amount grafted in these experiments falls into the narrow range (0.3–1.6 wt% Zr) published for zirconocene dichlorides immobilized on silica without the aid of base [36–39].

3.5. Characterization of supported catalysts

Besides determination of zirconium content by ICP-MS, all prepared complexes were characterized by TGA, IR spectroscopy and selected catalysts also by XPS.

The amount of zirconium incorporated in each catalyst (see Table 2) strongly depends on the starting material used and corresponding synthetic method. Not surprisingly, independently of the method of preparation, silica $SiO_{2(200)}$ with high concentration of surface groups (3.6 mmol–OH/g) as inorganic ligand/support afforded catalysts with higher Zr loading compared to silica $SiO_{2(500)}$ (0.7 mmol –OH/g). The use of stoichiometric

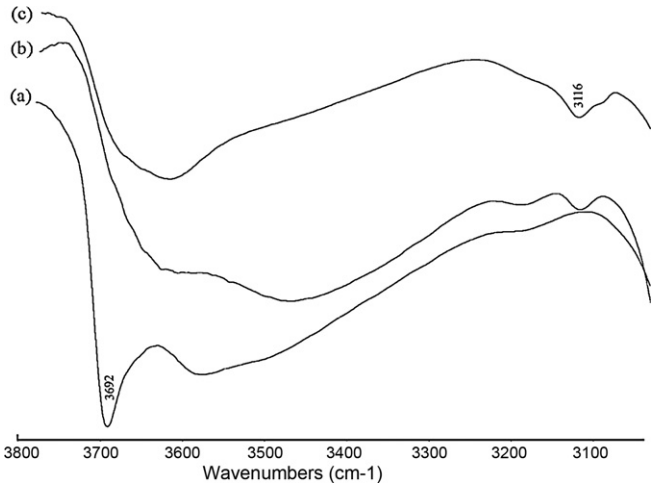

Fig. 3. FT-IR spectra of $SiO_{2(200)}$ (a); $SiO_{2(200)}/Cp_2ZrCl_2/NEt_3(7.8)$ (b); $SiO_{2(200)}/Cp_2ZrMe_2(9.5)$ (c).

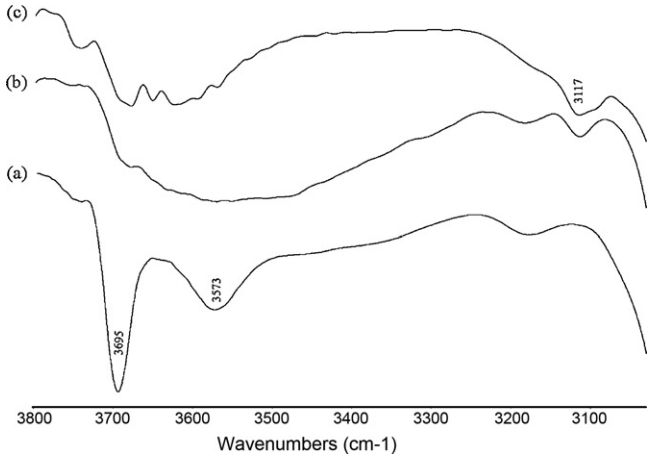

Fig. 4. FT-IR spectra of $SiO_{2(500)}$ (a); $SiO_{2(500)}/Cp_2ZrCl_2/NEt_3(5.8)$ (b); $SiO_{2(500)}/Cp_2ZrMe_2(7.5)$ (c).

or higher amount of zirconocene ($[(\eta^5\text{-}C_5H_5)_2ZrCl_2]$/surface –OH ≥ 1) for grafting on $SiO_{2(500)}$ in the presence NEt_3 (Method A) gave heterogeneous catalysts $SiO_{2(500)}/Cp_2ZrCl_2/NEt_3(5.3)$ and $SiO_{2(500)}/Cp_2ZrCl_2/NEt_3(5.8)$ where the molar amount of Zr (0.58 mmol/g for former and 0.64 mmol/g for latter) implied preferred formation of ≡SiO–$ZrClCp_2$ species on the surface. The molar ratio $[(\eta^5\text{-}C_5H_5)_2ZrCl_2]$/surface –OH (in $SiO_{2(500)}$) ~0.5 led to the catalyst $SiO_{2(500)}/Cp_2ZrCl_2/NEt_3(3.0)$ where an approximately half Zr loading in comparison to $SiO_{2(500)}/Cp_2ZrCl_2/NEt_3(5.8)$ was found and this led us to conclude that ≡SiO–$ZrClCp_2$ is also a predominant species in the $SiO_{2(500)}/Cp_2ZrCl_2/NEt_3(3.0)$, probably as a result of low concentration of –OH groups on the silica surface which precludes formation of chelating species $(\equiv SiO)_2\text{–}ZrCp_2$. The amount of zirconocene grafted (7.8 wt% Zr, i.e. 0.86 mmol/g for $SiO_{2(200)}/Cp_2ZrCl_2/NEt_3(7.8)$ and 8.7 wt% Zr, i.e. 0.96 mmol/g for $SiO_{2(200)}/Cp_2ZrCl_2/NEt_3(8.7)$) on silica $SiO_{2(200)}$ (3.6 mmol –OH/g) showed that the resulting catalyst should contain residual concentration of –OH groups (even when possible formation of chelating species ($(\equiv SiO)_2\text{–}ZrCp_2$ is kept in view). Preparation of grafted zirconocene catalysts $SiO_{2(200)}/Cp_2ZrMe_2(9.5)$ and $SiO_{2(500)}/Cp_2ZrMe_2(7.5)$ by Method B led to species with by far the highest Zr loading, obviously due to the high reactivity of $[(\eta^5\text{-}C_5H_5)_2ZrMe_2]$. Therein the zirconium loading (7.5 wt% of Zr, i.e. 0.8 mmol Zr/g catalyst) in $SiO_{2(500)}/Cp_2ZrMe_2(7.5)$ catalyst slightly exceeds the number of surface –OH groups in used silica $SiO_{2(500)}$ (0.7 mmol –OH groups/g). We suggested that the zirconocene moiety is grafted not only by acidobasic reaction between Zr–Me and ≡SiO–OH (giving ≡SiO–$ZrMeCp_2$ and methane), but also by the opening of strained siloxane bridges Si–O–Si (giving ≡SiO–$ZrMeCp_2$ and ≡SiO–Me) as was proved for reaction of $[(\eta^5\text{-}C_5Me_5)_2ZrMe_2]$ with highly dehydroxylated silica [40]. Method C led to catalyst $SiO_{2(200)}/Cp_2ZrCl_2(1.1)$ and $SiO_{2(500)}/Cp_2ZrCl_2(0.8)$ with negligible zirconium content showing low reactivity of Zr–Cl bond towards weekly acidic surface –OH groups [39].

FT-IR spectra of catalysts in the –OH stretching region (3200–3800 cm^{-1}) revealed that the peak at 3690–3695 cm^{-1} (terminal silanol groups) vanished after complexes were grafted onto both $SiO_{2(200)}$ (Fig. 3) and $SiO_{2(500)}$ (Fig. 4). This showed higher reactivity of the terminal silanol groups towards a Zr–Cl or Zr–Me bond in comparison to vicinal silanol groups [41,42]. Typical feature of catalyst spectra showing presence of the zirconocene moiety is a weak band at 3116–3120 cm^{-1} assigned to the valence C–H vibration of zirconocene cyclopentadienyl ring that is shifted to higher wavenumbers from that for $[(\eta^5\text{-}C_5H_5)_2ZrCl_2]$ (3102 cm^{-1}).

The thermogravimetric analysis (TGA) of the prepared catalysts were performed and curves of particular catalysts are depicted in Fig. 5. The first weight loss at 210–240 °C could be assigned to a release of cyclopentadienyl ligand from the supported catalyst. For catalyst $SiO_{2(500)}/Cp_2ZrCl_2/NEt_3(5.8)$ (Fig. 5a), where this weight loss does not overlap with other processes, a molar ratio C_5H_6/Zr ~1.64 could be calculated which is close to value expected for $(\eta^5\text{-}C_5H_5)_2Zr$ fragment. The weight loss with maximum at 330–350 °C (e.g. Fig. 5c) which is typical for TGA curve of catalysts $SiO_{2(200)}/Cp_2ZrCl_2/NEt_3(7.8)$ and $SiO_{2(200)}/Cp_2ZrCl_2/NEt_3(8.7)$ could be interpreted as a water elimination due to condensation of vicinal silanol groups.

A surface composition of particular heterogeneous catalysts $SiO_{2(500)}/Cp_2ZrCl_2/NEt_3(5.8)$, $SiO_{2(500)}/Cp_2ZrCl_2/NEt_3(3.0)$ and $SiO_{2(200)}/Cp_2ZrCl_2/NEt_3(7.8)$ and the metallocene binding energies was examined by XPS. The Zr $3d_{5/2}$ binding energies obtained were 182.2 eV for $SiO_{2(500)}/Cp_2ZrCl_2/NEt_3(5.8)$, 182.3 eV for $SiO_{2(500)}/Cp_2ZrCl_2/NEt_3(3.0)$ and 182.3 eV for $SiO_{2(200)}/Cp_2ZrCl_2/NEt_3(7.8)$, and differ only slightly from each other and also from the value published for $[(\eta^5\text{-}C_5H_5)_2ZrCl_2]$ (182.0 eV) and $[\{(\eta^5\text{-}C_5H_5)_2ZrCl\}O_2]$ (182.1 eV) [43]. The rather low sensitivity of Zr $3d_{5/2}$ binding energy to σ-ligand chlorine to silanolate exchange is in accordance with our previous finding of solely Zr $3d_{5/2}$ binding energy value (182.0 ± 0.1 eV) for dinuclear homogeneous complex **3b** containing two different zirconocene moieties [25]. The molar ratio C/Zr ~ 13.2 ($SiO_{2(500)}/Cp_2ZrCl_2/NEt_3(5.8)$), 11.9 ($SiO_{2(200)}/Cp_2ZrCl_2/NEt_3(7.8)$) and 14.0 ($SiO_{2(500)}/Cp_2ZrCl_2/NEt_3(3.0)$) established by XPS measurement is slightly higher than that expected for $(\eta^5\text{-}C_5H_5)_2Zr$ fragment (C/Zr = 10). The molar ratio Cl/Zr ~ 1 in catalyst $SiO_{2(200)}/Cp_2ZrCl_2/NEt_3(7.8)$ fitted well with the supposed surface species ≡SiO–$ZrClCp_2$. On the other hand in complexes $SiO_{2(500)}/Cp_2ZrCl_2/NEt_3(5.8)$ (Cl/Zr ~ 1.7) and $SiO_{2(500)}/Cp_2ZrCl_2/NEt_3(3.0)$ (Cl/Zr ~ 1.9) the molar Cl/Zr ratio significantly exceeds the expected value, although the catalysts were thoroughly washed in order to remove $[(\eta^5\text{-}C_5H_5)_2ZrCl_2]$. Unfortunately the origin of the adventitious chlorine is not clear to date. Finally, it should be noted that XPS analysis did not locate any nitrogen in the catalysts studied, therefore the physisorption of NEt_3 and/or $[NEt_3H]Cl$ on the catalysts surface can be excluded.

3.6. Catalytic phenylsilane polymerization with heterogeneous complexes

The heterogeneous zirconocene complexes were tested in the polymerization of phenylsilane under the same

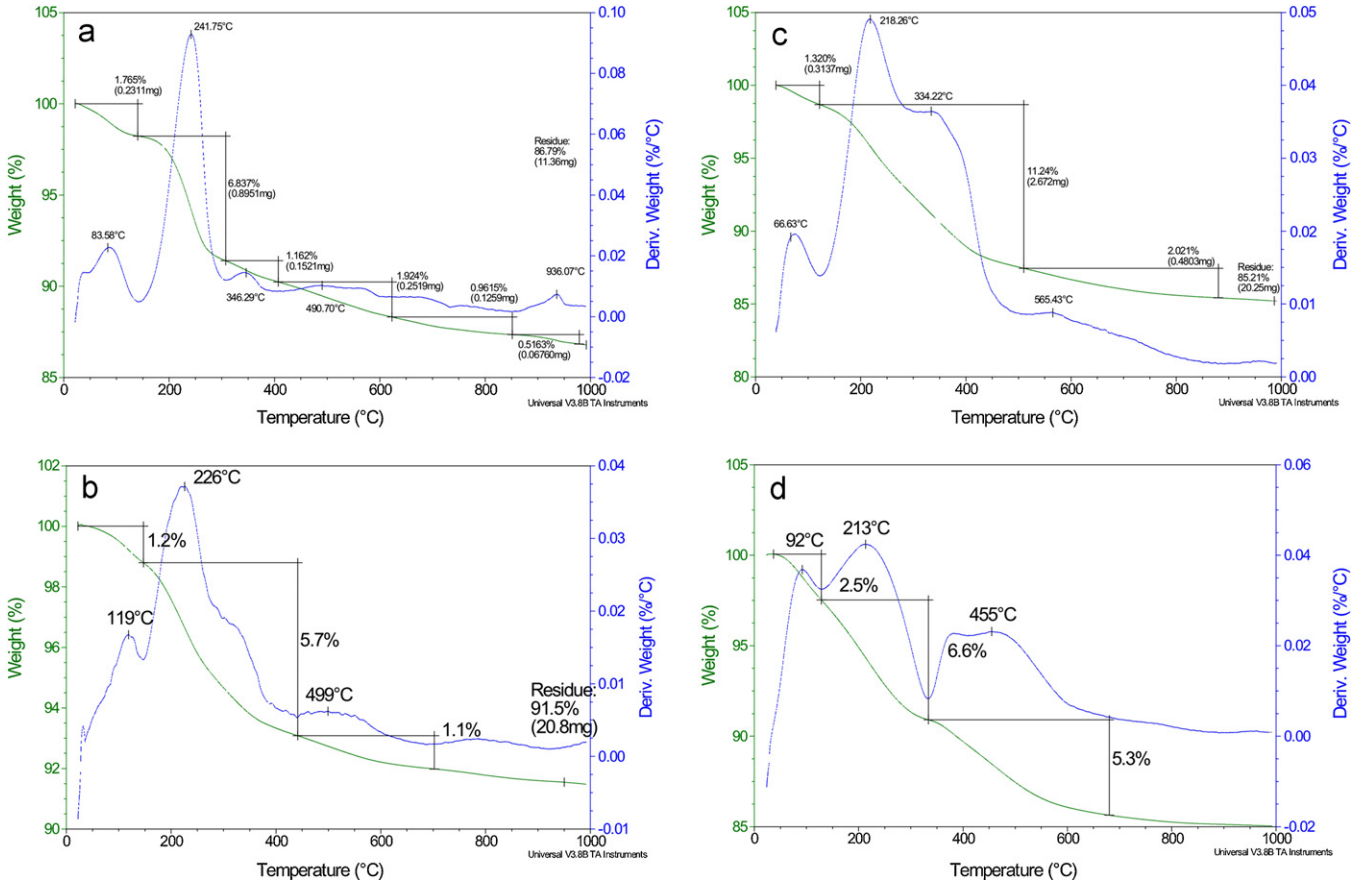

Fig. 5. TGA curves of $SiO_{2(500)}/Cp_2ZrCl_2/NEt_3(5.8)$ (a); $SiO_{2(500)}/Cp_2ZrCl_2/NEt_3(3.0)$ (b); $SiO_{2(200)}/Cp_2ZrCl_2/NEt_3(7.8)$ (c); $SiO_{2(200)}/Cp_2ZrMe_2(9.5)$ (d) acquired at 20 °C min $^{-1}$ under a flow of nitrogen.

conditions (temperature 105 °C, time 15 h, neat $PhSiH_3$) as the homogeneous analogues **1–5**, except for the Zr/$PhSiH_3$ ratio. The preliminary experiment with $SiO_{2(500)}/Cp_2ZrCl_2/NEt_3(5.8)$ catalyst at Zr/$PhSiH_3$ = 1/1000 (n/n) showed no polymerization at all, therefore a higher Zr loading (Zr/$PhSiH_3$ = 1/100; n/n) was used. The results of these experiments are shown in Table 2. The catalytic performance decreases in the order: $SiO_{2(500)}/Cp_2ZrMe_2(7.5) \sim SiO_{2(200)}/Cp_2ZrMe_2(9.5) \sim SiO_{2(500)}/Cp_2ZrCl_2/NEt_3(5.3) \sim SiO_{2(500)}/Cp_2ZrCl_2/NEt_3(5.8) > SiO_{2(500)}/Cp_2ZrCl_2/NEt_3(3.0) > SiO_{2(200)}/Cp_2ZrCl_2/NEt_3(8.7) \sim SiO_{2(200)}/Cp_2ZrCl_2/NEt_3(7.8) \gg SiO_{2(500)}/Cp_2ZrCl_2(0.8) \sim SiO_{2(200)}/Cp_2ZrCl_2(1.1)$ (the last two catalysts were found to be inactive). Reproducibility of polymerization is fair as could be seen from monomer conversions (81% and 69%) and M_w of the polymers obtained (3.61 kg mol^{-1} and 3.96 kg mol^{-1}) for the same catalyst (entries 3 and 4). Catalysts prepared by the same synthetic procedure (although containing slightly different Zr content) behave similarly in the polymerization reaction and produce polymers with similar characteristic. This could be demonstrated on catalyst prepared either from $SiO_{2(200)}$ – $SiO_{2(200)}/Cp_2ZrCl_2/NEt_3(8.7)$ and $SiO_{2(200)}/Cp_2ZrCl_2/NEt_3(7.8)$ (compare entries 5 and 6) or from $SiO_{2(500)}$–$SiO_{2(500)}/Cp_2ZrCl_2/NEt_3(5.3)$ and $SiO_{2(500)}/Cp_2ZrCl_2/NEt_3(5.8)$ (compare entries 1 and 2).

The productivity of catalysts prepared by method A bearing $SiO_{2(500)}$ – $SiO_{2(500)}/Cp_2ZrCl_2/NEt_3(5.3)$ and $SiO_{2(500)}/Cp_2ZrCl_2/NEt_3(5.8)$ (entries 1 and 2) is twice as high compared to catalysts bearing $SiO_{2(200)}$: $SiO_{2(200)}/Cp_2ZrCl_2/NEt_3(8.7)$ and $SiO_{2(200)}/Cp_2ZrCl_2/NEt_3(7.8)$ (entries 5 and 6) and the former two catalysts also produce polysilanes with higher M_w (4.01 (entry 1), 3.70 (entry 2) vs. 1.20 (entry 5), 0.89 (entry 6) kg mol^{-1}) than the latter one. The considerably lower productivity of the latter catalysts is probably a consequence of higher concentration of residual surface –OH groups which act as terminating agents for generated active species. Complexes prepared by Method C ($SiO_{2(500)}/Cp_2ZrCl_2(0.8)$ and $SiO_{2(200)}/Cp_2ZrCl_2(1.1)$) possessed even higher content of surface silanol groups (in comparison to Zr content) which eventually led to efficient grafting of active species and their deactivation (entries 9 and 10).

Both catalysts ($SiO_{2(500)}/Cp_2ZrMe_2(7.5)$ and $SiO_{2(200)}/Cp_2ZrMe_2(9.5)$) prepared by method B from [(η^5-$C_5H_5)_2ZrMe_2$] precursor displayed high catalytic performance (entries 7 and 8). In this respect the higher activity of the latter catalyst bearing $SiO_{2(200)}$ compared to similar catalysts based on method A (e.g. $SiO_{2(200)}/Cp_2ZrCl_2/NEt_3(7.8)$) arise probably from easier formation of the active species due to a higher reactivity of Zr–Me bond in comparison to Zr–Cl bond rather than from a high zirconium content.

3.7. Recycling of heterogeneous catalysts $SiO_{2(500)}/Cp_2ZrCl_2/NEt_3(5.8)$ and $SiO_{2(200)}/Cp_2ZrCl_2/NEt_3(7.8)$

A large recovery of homogeneous catalyst **1a** from the polymerization mixture showed its incomplete activation in the polymerization. This led us to test the heterogeneous catalysts as a source of active species for repeated phenylsilane polymerization. The results of three consecutive phenylsilane polymerization cycles catalyzed with $SiO_{2(500)}/Cp_2ZrCl_2/NEt_3(5.8)$ are summarized in Table 3. The Zr content decreased a little (from initial 5.8% to final 4.7%) causing only a slight decrease in catalytic performance. Moreover the polysilanes produced are almost identical as could be seen from their GPC (Fig. 6) and NMR characterization (Fig. 7). The reusability of $SiO_{2(200)}/Cp_2ZrCl_2/NEt_3(7.8)$ in phenylsilane poly-

Table 3
Recycling of $SiO_{2(500)}/Cp_2ZrCl_2/NEt_3$(5.8) catalyst in polymerization of phenylsilane. Conditions: $Zr/PhSiH_3$ = 1/100; temp. = 105 °C; time = 15 h; neat $PhSiH_3$.

Cycle	Zr loading (wt%)[a]	Conv. [%]	M_w[b]	D[b,c]	LMF[b,d] [mol%]
1st	5.8	91	3.70	1.69	9
2nd	5.4	98	3.84	1.70	9
3rd	4.7[e]	86	3.82	1.76	10

[a] Determined by ICP-MS.
[b] Determined by GPC-MALLS.
[c] Dispersity $D = M_w/M_n$.
[d] Low molecular weight fraction.
[e] Zr loading after the 3rd cycle was 4.7 wt%.

Table 4
Recycling $SiO_{2(200)}/Cp_2ZrCl_2/NEt_3$(7.8) catalyst in polymerization of phenylsilane. Conditions: $Zr/PhSiH_3$ = 1/100; temp. = 105 °C; time = 15 h; neat $PhSiH_3$.

Cycle	Zr loading (wt%)[a]	Conv. [%]	M_w[b]	D[b,c]	LMF[b,d] [mol%]
1st	7.8	45	1.20	2.22	68
2nd	7.8	80	3.35	1.66	9
3rd	7.7[e]	81	3.13	1.63	15

[a] Determined by ICP-MS.
[b] Determined by GPC-MALLS.
[c] Dispersity $D = M_w/M_n$.
[d] Low molecular weight fraction.
[e] Zr loading after the 3rd cycle was 7.1 wt%.

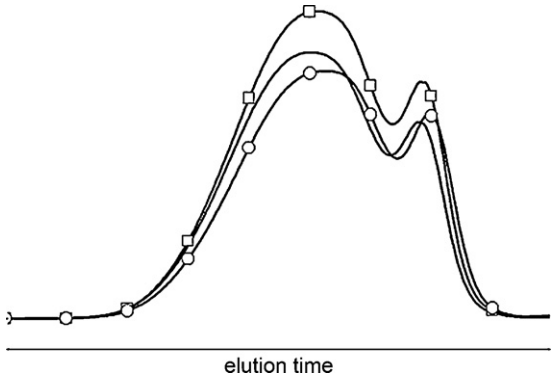

Fig. 6. GPC of polyphenylsilanes prepared by recycled $SiO_{2(500)}/Cp_2ZrCl_2/NEt_3$(5.8) catalyst. 1st cycle (—), 2nd cycle (—□—) and 3rd cycle (—○—).

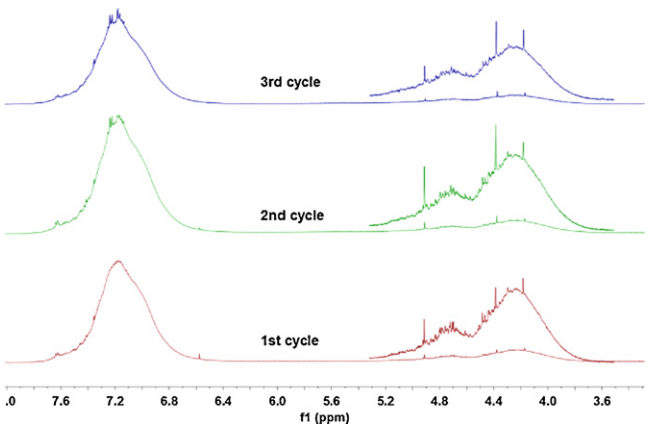

Fig. 7. ^{1}H NMR spectra of polyphenylsilanes (in $(CD_3)_2CO$) prepared by recycled $SiO_{2(500)}/Cp_2ZrCl_2/NEt_3$(5.8) catalyst. 1st cycle (bottom), 2nd cycle (middle) and 3rd cycle (top).

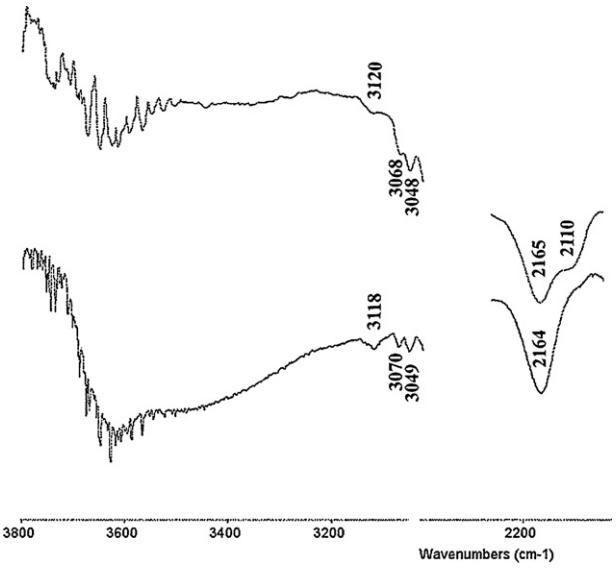

Fig. 8. FT-IR spectra of catalysts after 3rd polymerization cycle: $SiO_{2(500)}/Cp_2ZrCl_2/NEt_3$(5.8) (top); $SiO_{2(200)}/Cp_2ZrCl_2/NEt_3$(7.8) (bottom).

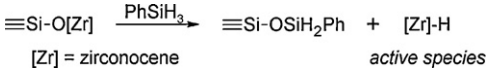

Scheme 1.

merization was also checked and the results are summarized in Table 4. The catalysts showed a twofold increase in monomer conversion in the second polymerization cycle compared to first one and then the conversion remained unchanged in the third cycle. Similarly, M_w value of the resulting polymer increased significantly in the second cycle and then changed only slightly in the last one. A possible explanation of the improved catalyst performance in the second cycle could arise from capping of residual free silanol groups on the catalyst surface by phenylsilane during the first cycle. This might prevent the deactivation of the active species, explaining thus the increased overall catalytic performance.

The zirconocene framework was partially preserved in both recycled catalysts after its last use as was demonstrated by the presence of ν(C–H) band of cyclopentadienyl ring at 3118–3120 cm^{-1} in the FT-IR spectra (Fig. 8). This assumption was further supported by XPS analysis of reused $SiO_{2(500)}/Cp_2ZrCl_2/NEt_3$(5.8) where the value obtained for Zr $3d_{5/2}$ binding energy (182.3 eV) is equal to that obtained for bare $SiO_{2(500)}/Cp_2ZrCl_2/NEt_3$(5.8) (182.3 eV). On the other hand, the decreased Zr content (see Tables 3 and 4) in reused catalyst clearly shows that zirconium is partially leached from silica surface. Moreover, new bands at 3070 and 3050 cm^{-1} belonging to a phenyl group and the ν(Si–H) characteristic band at 2164–2165 cm^{-1} (with a shoulder at ca. 2110 cm^{-1}) were found in the FT-IR spectra (Fig. 8) of reused catalysts. With respect to these findings we propose the activation of the heterogeneous catalysts by a cleave of a Zr–O bond with phenylsilane and subsequent releasing of active homogeneous hydride zirconocene species as depicted in Scheme 1. Phenylsilane is then grafted on the silica with concomitant formation of surface species $\equiv Si–OSiH_2Ph$. This mechanism of activation is in accordance to σ-ligand transfer from homogeneous complexes $[(\eta^5\text{-}C_5H_5)_2ZrY_2]$ (Y = F, OPh, NMe_2; M_w = 2.70–3.14 kg mol^{-1}) to primary, secondary and tertiary silanes as founded by Wang et al. [17].

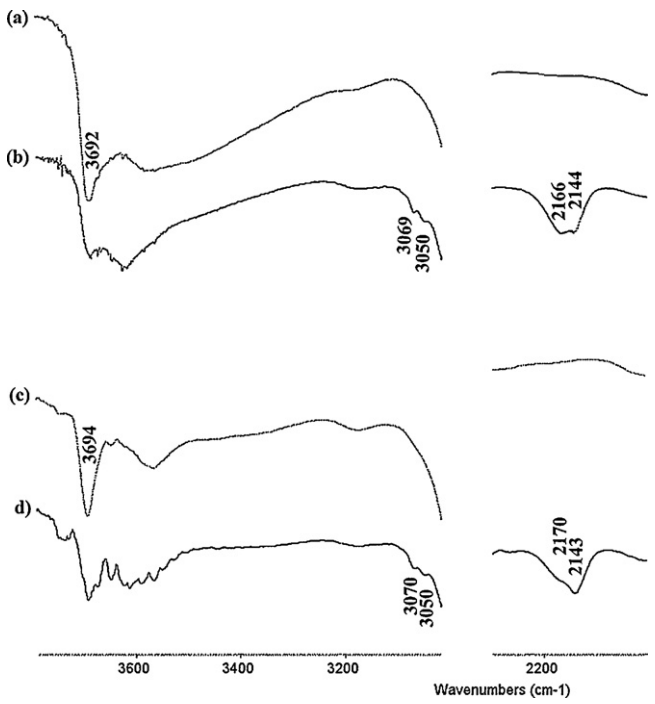

Fig. 9. FT-IR spectra of $SiO_{2(200)}$ (a); $SiO_{2(200)}/PhSiH_3$ (b); $SiO_{2(500)}$ (c); $SiO_{2(500)}/PhSiH_3$ (d).

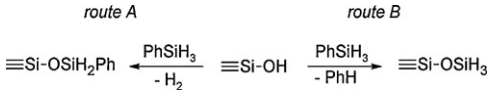

Scheme 2.

3.8. Reaction of neat $PhSiH_3$ with silica surface silanol groups

The treatments of $PhSiH_3$ with silicas $SiO_{2(500)}$ and $SiO_{2(200)}$ were performed in order to elucidate its reactivity towards surface silanol groups. The reaction gave silane modified silicas $SiO_{2(500)}/PhSiH_3$ and $SiO_{2(200)}/PhSiH_3$ at the temperature used for phenylsilane polymerization. Analysis of the FT-IR spectra (Fig. 9) of both modified silica materials revealed the diminution of free silanol vibration at 3690–3695 cm^{-1} in comparison to bare silicas. In addition, peaks at 3070 and 3050 cm^{-1} (valence C–H vibrations of aromatic group) and a composite peak with maxima at 2166–2170 cm^{-1} and 2143–2144 cm^{-1} (region characteristic for ν(Si–H)) were found in the spectra. This leads us to propose two possible pathways (Scheme 2) for reaction of phenylsilane with silanol groups at a silica surface. In route A the surface species $\equiv Si–OSiH_2Ph$ is formed by "acidobasic" reaction where phenylsilane acts as an organometallic hydride and hydrogen gas is released as a byproduct. Bansleben et al. mentioned that the reaction is preferred in the presence of equimolar amount of triethylamine, whereas the phenylsilane-modified silica obtained resembled ν(Si–H) at 2178 cm^{-1} in DRIFT IR spectra [44]. Therefore the ν(Si–H) vibration found at 2166–2170 cm^{-1} in $SiO_{2(500)}/PhSiH_3$ and $SiO_{2(200)}/PhSiH_3$ could be most probably assigned to surface species $\equiv Si–OSiH_2Ph$ as was shown above for reused catalysts $SiO_{2(500)}/Cp_2ZrCl_2/NEt_3$(5.8) and $SiO_{2(200)}/Cp_2ZrCl_2/NEt_3$(7.8). The proposed route B is based on a recently found dearylation of arylsilanes (Aryl = Ph [45]; Aryl = 4-Me-C_6H_4, 4-OMe-C_6H_4, 4-CF_3-C_6H_4 [46]) promoted by acidic silanol groups on the silica surface and accompanied by grafting of silane on the silica surface. According to route B, the reaction of the phenylsilane with free silanol could constitute surface species $\equiv Si–OSiH_3$ and benzene. Indeed, benzene was detected by GC–MS analysis of the reaction solutions. The absorption found at 2144 cm^{-1} in $SiO_{2(500)}/PhSiH_3$ and $SiO_{2(200)}/PhSiH_3$ could be tentatively assigned to ν(Si–H) vibration of such $\equiv Si–OSiH_3$ species. The decrease of ν(Si–H) frequency in $\equiv Si–OSiH_3$ species compared to $\equiv Si–OSiH_2Ph$ species is consistent with formal replacing of electron-attracting phenyl group by electron-donating hydride atom. The route B takes part probably only in the presence of more acidic free (terminal, isolated) surface silanol groups as we did not observe the band at 2144 cm^{-1} in the IR-spectra of the reused catalysts.

4. Conclusions

Initial catalytic phenylsilane polymerization tests with homogeneous zirconocene complexes showed that the presence of silanol ligand is crucial for high catalyst performance. The ^1H and ^{29}Si NMR monitoring of polymerization catalyzed with **1a** proved that only a small amount of active species is generated from the parent complex during the activation step. On the other hand, once the active species is formed it persists without deactivation for a couple of hours and catalyzed the dehydrocoupling polymerization with high efficiency. We propose that its low concentration in the reaction mixture lowers its deactivation by a bimolecular reaction which could lead to an inactive dimer. The silica grafted heterogeneous catalysts were found also to be efficient in the phenylsilane polymerization although a higher Zr/monomer ratio had to be used in comparison with homogeneous analogues. The low concentration of residual silanol groups in heterogeneous catalysts was found essential for high catalytic performance, most probably due to the ability of silanol groups to quench the active species. The particular catalyst $SiO_{2(500)}/Cp_2ZrCl_2/NEt_3$(5.8) was used repeatedly (in three consecutive cycles) without loss of productivity and produced polymers with almost identical properties. To the best of our knowledge, this is the first example of group 4 reusable catalyst for dehydrogenative coupling of phenylsilane. The analyses of the reused catalysts showed, that an active zirconium–hydride species is released from silica surface by cleavage of ≡SiO–Zr bond by hydride transferred from phenylsilane. A slight decrease of zirconium loading in the catalyst after repeated polymerization experiments implies that these catalysts should be regarded as a long-lasting source of soluble catalytically active hydride species rather than a true heterogeneous catalyst.

Acknowledgements

Authors wish to thank to Dr. Arnošt Zukal for silica surface area measurement, Prof. Oto Mestek for Zr loading determinations in supported catalysts (ICP-MS) and Dr. Jana Kredatusová for TGA. J.P. thanks to Dr. Karel Mach (J. H. Inst. Phys. Chem.) for helpful discussion. The financial support from the Academy of Sciences of the Czech Republic (projects GA203/09/1574 and KAN100400701) is gratefully acknowledged. I.C. is grateful to MSM0021620857.

References

[1] R. West, J. Organomet. Chem. 300 (1986) 327.
[2] R.D. Miller, J. Michl, Chem. Rev. 89 (1989) 1359.
[3] J.F. Harrod, Coord. Chem. Rev. 206 (2000) 493.
[4] J.Y. Corey, In Advances in Organometallic Chemistry Vol 51, Academic Press Inc, San Diego, 2004, 1.
[5] T.J. Clark, K. Lee, I. Manners, Chem. -Eur. J 12 (2006) 8634.
[6] E. Samuel, J.F. Harrod, J. Am. Chem. Soc. 106 (1984) 1859.
[7] Y. Mu, C. Aitken, B. Cote, J.F. Harrod, E. Samuel, Can. J. Chem.-Rev. Can. Chim. 69 (1991) 264.
[8] J.Y. Corey, J. Braddock-Wilking, Chem. Rev. 99 (1999) 175.
[9] J.Y. Corey, Chem. Rev. 111 (2011) 863.
[10] J.Y. Corey, X.H. Zhu, J. Organomet. Chem. 439 (1992) 1.
[11] J.Y. Corey, X.H. Zhu, T.C. Bedard, L.D. Lange, Organometallics 10 (1991) 924.

[12] H.G. Woo, S.Y. Kim, M.K. Han, E.J. Cho, I.N. Jung, Organometallics 14 (1995) 2415.
[13] V.K. Dioumaev, J.F. Harrod, Organometallics 16 (1997) 1452.
[14] R.J.P. Corriu, M. Enders, S. Huille, J.J.E. Moreau, Chem. Mater. 6 (1994) 15.
[15] S. Bourg, R.J.P. Corriu, M. Enders, J.J.E. Moreau, Organometallics 14 (1995) 564.
[16] F. Lunzer, C. Marschner, S. Landgraf, J. Organomet. Chem. 568 (1998) 253.
[17] Q.Z. Wang, J.Y. Corey, Can. J. Chem.-Rev. Can. Chim. 78 (2000) 1434.
[18] W.W. Lukens, M.R. Smith, R.A. Andersen, J. Am. Chem. Soc. 118 (1996) 1719.
[19] V. Varga, I. Císařová, R. Gyepes, M. Horáček, J. Kubišta, K. Mach, Organometallics 28 (2009) 1748.
[20] R. Gyepes, V. Varga, M. Horáček, J. Kubišta, J. Pinkas, K. Mach, Organometallics 29 (2010) 3780.
[21] X. Solans-Monfort, J.-S. Filhol, C. Coperet, O. Eisenstein, New J. Chem. 30 (2006) 842.
[22] J.C.W. Chien, Top. Catal. 7 (1999) 23.
[23] C. Coperet, M. Chabanas, R.P. Saint-Arroman, J.M. Basset, Angew. Chem.-Int. Edit. 42 (2003) 156.
[24] J.R. Severn, J.C. Chadwick, R. Duchateau, N. Friederichs, Chem. Rev. 105 (2005) 4073.
[25] V. Varga, J. Pinkas, R. Gyepes, P. Štěpnička, M. Horáček, Z. Bastl, K. Mach, Collect. Czech. Chem. Commun. 75 (2010) 105.
[26] K. Wada, M. Bundo, D. Nakabayashi, N. Itayama, T. Kondo, T. Mitsudoh, Chem. Lett. (2000) 628.
[27] M.D. Skowronska-Ptasinska, R. Duchateau, R.A. van Santen, G.P.A. Yap, Organometallics 20 (2001) 3519.
[28] K.L. Fujdala, A.G. Oliver, F.J. Hollander, T.D. Tilley, Inorg. Chem. 42 (2003) 1140.
[29] G.M. Sheldrick, SHELXL97, Program for Crystal Structure Refinement from Diffraction Data, University of Göttingen, Göttingen, 1997.
[30] P.W. Betteridge, J.R. Carruthers, R.I. Cooper, K. Prout, D.J. Watkin, J. Appl. Cryst. 36 (2003) 1487.
[31] E. Samuel, Bull. Soc. Chim. Fr. (1966) 3548.
[32] M. Horáček, J. Merna, R. Gyepes, J. Sýkora, J. Kubišta, J. Pinkas, Collect. Czech. Chem. Commun. 76 (2011) 75.
[33] V.K. Dioumaev, K. Rahimian, F.o. Gauvin, J.F. Harrod, Organometallics 18 (1999) 2249.
[34] T. Takahashi, M. Hasegawa, N. Suzuki, M. Saburi, C.J. Rousset, P.E. Fanwick, E. Negishi, J. Am. Chem. Soc. 113 (1991) 8564.
[35] F.J. Feher, D.A. Newman, J.F. Walzer, J. Am. Chem. Soc. 111 (1989) 1741.
[36] L. Britcher, H. Rahiala, K. Hakala, P. Mikkola, J.B. Rosenholm, Chem. Mater. 16 (2004) 5713.
[37] J.H.Z. dos Santos, C. Krug, M.B. da Rosa, F.C. Stedile, J. Dupont, M.D. Forte, J. Mol. Catal. A-Chem. 139 (1999) 199.
[38] J.H.Z. dosSantos, S. Dorneles, F.C. Stedile, J. Dupont, M.M.D. Forte, I.J.R. Baumvol, Macromol. Chem. Phys. 198 (1997) 3529.
[39] C. Alonso, A. Antinolo, F. Carrillo-Hermosilla, P. Carrion, A. Otero, J. Sancho, E. Villasenor, J. Mol. Catal. A-Chem. 220 (2004) 285.
[40] C.P. Nicholas, H.S. Ahn, T.J. Marks, J. Am. Chem. Soc. 125 (2003) 4325.
[41] N.G. Dufrenne, J.P. Blitz, C.C. Meverden, Microchem. J. 55 (1997) 192.
[42] S. Haukka, A. Root, J. Phys. Chem. 98 (1994) 1695.
[43] F. Garbassi, L. Gila, A. Proto, J. Mol. Catal. A-Chem. 101 (1995) 199.
[44] D.A. Bansleben, E.F. Connor, R.H. Grubbs, J.I. Henderson, A.R. Nadjadi Jr., T.R. Younkin, US6197714 2001, Cryovac, Inc., Duncan, SC.
[45] S. Lipponen, M. Lahelin, J. Seppala, Eur. Polym. J. 45 (2009) 1179.
[46] N. Fukaya, H. Haga, T. Tsuchimoto, S. Onozawa, T. Sakakura, H. Yasuda, J. Organomet. Chem. 695 (2010) 2540.